Arrays of Dual Nanomechanical Resonators for Selective Biological Detection

ARTICLE *in* ANALYTICAL CHEMISTRY · APRIL 2009

Impact Factor: 5.64 · DOI: 10.1021/ac8024152 · Source: PubMed

7 AUTHORS, INCLUDING:

María Arroyo-Hernández
Universidad Politécnica de Madrid
21 PUBLICATIONS **188** CITATIONS
SEE PROFILE

Tong Duy Hien
Nanosens
55 PUBLICATIONS **901** CITATIONS
SEE PROFILE

C.J.M. van Rijn
Wageningen University
108 PUBLICATIONS **1,840** CITATIONS
SEE PROFILE

Montserrat Calleja
Spanish National Research Council
72 PUBLICATIONS **2,054** CITATIONS
SEE PROFILE

Article

Arrays of Dual Nanomechanical Resonators for Selective Biological Detection

Daniel Ramos, Mari#a Arroyo-Herna#ndez, Eduardo Gil-Santos, Hien Duy Tong, Cees Van Rijn, Montserrat Calleja, and Javier Tamayo

Anal. Chem., **2009**, 81 (6), 2274-2279• DOI: 10.1021/ac8024152 • Publication Date (Web): 17 February 2009

Anal. Chem. **2009,** *81,* 2274–2279

Arrays of Dual Nanomechanical Resonators for Selective Biological Detection

Daniel Ramos,[†] María Arroyo-Hernández,[†] Eduardo Gil-Santos,[†] Hien Duy Tong,[‡] Cees Van Rijn,[‡] Montserrat Calleja,[†] and Javier Tamayo*[,†]

Institute of Microelectronics of Madrid (IMM-CNM, CSIC), Isaac Newton 8 (PTM), Tres Cantos, 28760 Madrid, Spain, and Nanosens, Berkelkade 11, NL 7201 JE Zutphen, The Netherlands

Arrays of small nanomechanical resonators with dual geometry have been fabricated for sensitive biological detection. The arrays consist of silicon nitride resonating 100 nm thick cantilevers with sensing gold areas alternately placed on the free and fixed cantilever ends. The Au areas act as sensing regions as can be functionalized by means of thiol chemistry. The nanomechanical arrays provide a double flavor of the adsorbed molecules: the added mass reported by the cantilevers with the Au area at the tip and the nanoscale elasticity reported by the cantilevers with the Au area at the clamp. The devices were applied for DNA detection based on Watson−Crick pairing rules. The proposed design for nanomechanical resonators provides higher specificity for DNA sensing in comparison with conventional single cantilevers. The nanoscale elasticity induced by the DNA hybridization arises from the intermolecular interactions between the adsorbates bound to the cantilever and the surface stress.

The development of biosensors with high sensitivity and high selectivity remains of paramount importance in diverse fields, such as biology, healthcare, and food technology. Multidisciplinary research on nanotechnology has provided ultrasensitive nanobiosensors with a higher degree of miniaturization.[1−4] Among them, nanomechanical resonators have a huge potential for ultrasensitive detection of biomolecules.[4−9] The basic concept of these sensors is simple: when an object lands on a vibrating cantilever, its resonant frequency decreases by an amount that is proportional to the mass of the object. Since the sensitivity is inversely proportional to the active mass of the cantilever, the increasing ability to fabricate smaller cantilevers has made possible the weighing of minute adsorbed masses, even with subattogram resolution.[10] However, the attainment of this sensitivity for biosensing applications has been hindered because molecular recognition occurs in aqueous solutions, where the quality factor (Q) is extremely low due to the viscous damping.[11−13] An approach to circumvent this limitation considers measuring the change of the resonance frequency of simple nanomechanical resonators such as cantilevers in vacuum before and after immersion of the resonator in the biomolecule solution of interest.[5−7] Usually, the biomolecular receptors are immobilized along the entire cantilever or near the cantilever tip to maximize the mass sensitivity. Although, the mass sensitivity is at the attogram level, the specificity is severally degraded by the nonspecific adsorption and the contamination of the cantilever surface during the rinsing and drying steps.

Here, we have fabricated arrays of resonant ultrathin cantilevers, in which small sensing gold areas are alternately placed at the fixed and free cantilever ends. The concept is to propose the combination of several geometries in nanomechanical resonator arrays to enhance the specificity. In addition, these nanomechanical structures serve to gain major insight about the response of ultrathin nanomechanical resonators to biological adsorption.

METHODS

Cantilever Fabrication. A 4 in., 380 μm thick, double side polished ⟨100⟩-Si wafer is coated with 300 nm of wet-thermal silicon dioxide (SiO_2) and 100 nm of low-stress silicon-rich silicon nitride (SiN) by means of low-pressure chemical vapor deposition (LPCVD). A first microlithography procedure was then carried out to define the cantilever patterns on a photoresist layer on the front side of the wafer, followed by a dry ($CHF_3 + O_2$) etching of the SiN to etch the exposed silicon nitride film. This etching step is controlled to stop on the SiO_2 film. Afterward, the photoresist was stripped in an oxygen plasma. Subsequently, the second microlithography procedure, followed

* To whom correspondence should be addressed. E-mail: jtamayo@imm.cnm.csic.es.

[†] Institute of Microelectronics of Madrid.

[‡] Nanosens.

(1) Cheng, M.-C.; Cuda, G.; Bunimovich, Y. L.; Gaspari, M.; Heath, J. R.; Hill, H. D.; Mirkin, C. A.; Nijdam, A. J.; Terracciano, R.; Thundat, T.; Ferrari, M. *Curr. Opin. Chem. Biol.* **2006**, *10*, 11–19.

(2) Mertens, J.; Rogero, C.; Calleja, M.; Gago, J. M.; Briones, C.; Tamayo, J. *Nat. Nanotechnol.* **2008**, *3*, 301–307.

(3) Lavrik, N. V.; Sepaniak, M. J.; Datskos, P. G. *Rev. Sci. Instrum.* **2004**, *75*, 2229–2253.

(4) Waggoner, P. S.; Craighead, H. G. *Lab Chip* **2007**, *7*, 1238–1255.

(5) Ilic, B.; Yang, Y.; Aubin, K.; Reichenbach, R.; Krylov, S.; Craighead, H. G. *Nano Lett.* **2005**, *5*, 925–929.

(6) Gupta, A.; Akin, D.; Bashir, R. *Appl. Phys. Lett.* **2004**, *84*, 1976–1978.

(7) Varshney, M.; Waggoner, P. S.; Tan, C. P.; Aubin, K.; Montagna, R. A.; Craighead, H. G. *Anal. Chem.* **2008**, *80*, 2141–2148.

(8) Burg, T. P.; Manalis, S. R. *Appl. Phys. Lett.* **2003**, *83*, 2698–2700.

(9) Burg, T. P.; Godin, M.; Knudsen, S. M.; Shen, W.; Carlson, G.; Foster, J. S.; Babcock, K.; Manalis, S. R. *Nature* **2007**, *446*, 1066–1069.

(10) Yang, Y. T.; Callegari, C.; Feng, X. L.; Ekinci, K. L.; Roukes, M. L. *Nano Lett.* **2006**, *6*, 583–586.

(11) Sader, J. E. *J. Appl. Phys.* **1998**, *84*, 64–66.

(12) Braun, T.; Barwich, V.; Ghatkesar, M. K.; Bredekamp, A. H.; Gerber, C.; Hegner, M.; Lang, H. P. *Phys. Rev. E* **2005**, *72*, 031907.

(13) Ramos, D.; Mertens, J.; Calleja, M.; Tamayo, J. *Appl. Phys. Lett.* **2008**, *92*, 173108.

10.1021/ac8024152 CCC: $40.75
Published on Web 02/17/2009

by e-beam metal evaporation, and standard lift-off technique were carried out to pattern the Au areas on the cantilevers. The evaporated Au film had a thickness of 20 nm with an adhesion layer of 5 nm thick chromium. Then, windows were aligned and created on the back side of the wafer by the third microlithography procedure, followed by a through-wafer dry etching step (using a Bosch process with a SF_6/O_2 gas mixture). This through-wafer etching is controlled to stop when a sacrificial film of SiO_2 is reached. The front side (Au and nitride films) was protected during the dry etching procedure by a photoresist layer. Next, the photoresist film was stripped in an oxygen plasma oven, followed by wet etching of the SiO_2 layer in a diluted buffered oxide etch solution to reveal the free-standing silicon nitride cantilevers with Au areas at their free or fixed ends. It should be noted that the cantilever wafer was transferred directly from the wet-etch solution into a beaker containing distilled water and several surfactants to reduce surface tension. This procedure drastically improves the fabrication yield from about 50% (without this step) up to 90%. Finally, the wafer was manually separated into single chips with dimensions of 3 mm by 1.7 mm containing 25 cantilever beams.

Resonance Frequency and Surface Stress Measurements. The cantilever resonance frequency was measured in air by using the optical beam deflection technique. The beam from a green laser diode (1 mW, 532 nm, purchased from Edmund Optics) was tightly focused on the cantilever end by means of a beam expander and a long-working-distance objective (Mitutoyo Ltd.). The reflected beam was collected by a segmented photodetector (Hamamatsu) placed near the cantilevers. The differential photodetector signal has a significant contribution from the Brownian cantilever motion that allows detecting the resonance frequency by performing a Fourier transform. Importantly, optical inspection was performed after each adsorption experiment in order to check if the surface of the cantilevers was contaminated with salt debris or other particles that could produce artifacts in the measurements.

For measuring the surface stress, we measure the change of cantilever curvature by using an optical scanning technique previously described elsewhere.[2] In this case, we use gold-coated monocrystalline silicon microcantilever arrays purchased from Mikromasch. Microcantilevers were 400 μm long, 100 μm wide, and 1.0 μm thick.

DNA Experiments. ssDNA thiol-modified probes (with the 5′ modification $HS-(CH_2)_6$) and label-free ssDNA targets were obtained from Microsynth (Switzerland). DNA oligomers were HPLC-purified and desiccated. Prior to use, the samples were resuspended in PBS buffer (137 mM NaCl, 2.7 mM KCl, 8 mM Na_2HPO_4, 2 mM KH_2PO_4; pH = 7.5) and divided in aliquots of the desired volume at a concentration of 1 μM without further modifications. The cantilevers arrays were conjugated with a 16mer single-stranded DNA (5′-CTACCTTTTTTTTCTG-3′) derivatized with a thiol linker at the 5′ end that strongly binds to the gold. The immobilization time was about 20 h. Then the cantilevers were sequentially exposed to a noncomplementary ssDNA (5′-AGCTTCCGTACTCGAT-3′) and the complementary ssDNA, respectively. After each adsorption step, the cantilevers were vigorously rinsed in PBS and Milli-Q water (18 MΩ/cm) to remove weakly adsorbed molecules and dried under a stream of dry nitrogen gas. The fluorescence measurements were made using a Confocal MicroRadiance (Bio-Rad) coupled to a vertical Axioskop 2 microscope (Zeiss). The functionalized cantilevers were exposed to noncomplementary and complementary ssDNA labeled with fluorescein isothiocyanate at the 5′ end (Microsynth, Switzerland).

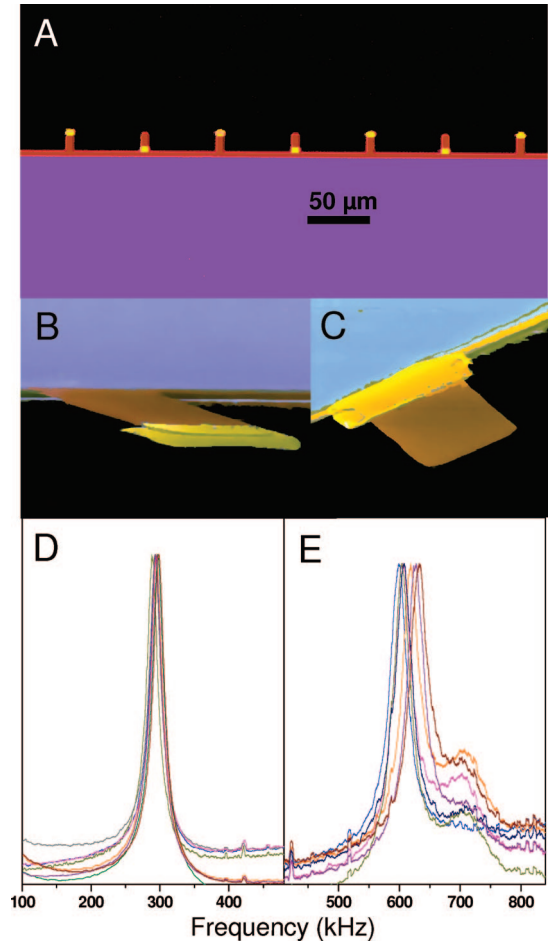

Figure 1. (A) Optical image of the array of nanomechanical sensors. (B and C) Scanning electron microscopy images of a cantilever with the Au area at the tip (B) and a cantilever with the Au area at the fixed end (C). (D and E) Frequency spectra of the Brownian motion of the cantilevers with the Au paddle at the tip (D) and at the fixed end (E). The spectra show the resonance peaks of the cantilevers.

RESULTS AND DISCUSSION

Concept of Dual Configuration in the Nanomechanical Resonator Array. Figure 1A–C shows images of the fabricated arrays of dual nanomechanical resonators. The cantilevers are 15 μm long, 6 μm wide, 100 nm thick, and with a cantilever pitch of 60 μm. The resonance frequency of the cantilevers was measured in air from the Brownian fluctuations by the optical beam deflection technique. The cantilevers with the gold area on the free end exhibited a resonance frequency of about 310 kHz (Figure 1D), whereas the cantilevers with the Au area on the fixed end had a resonance frequency of about 650 kHz (Figure 1E). The quality factors were 25–30 in air. The resonance frequency deviation between the cantilevers in the same array was of about 0.8%. The high number of cantilevers per chip, 25, and the uniformity in the mechanical properties of the cantilevers allow for a meaningful statistics of the measurements.

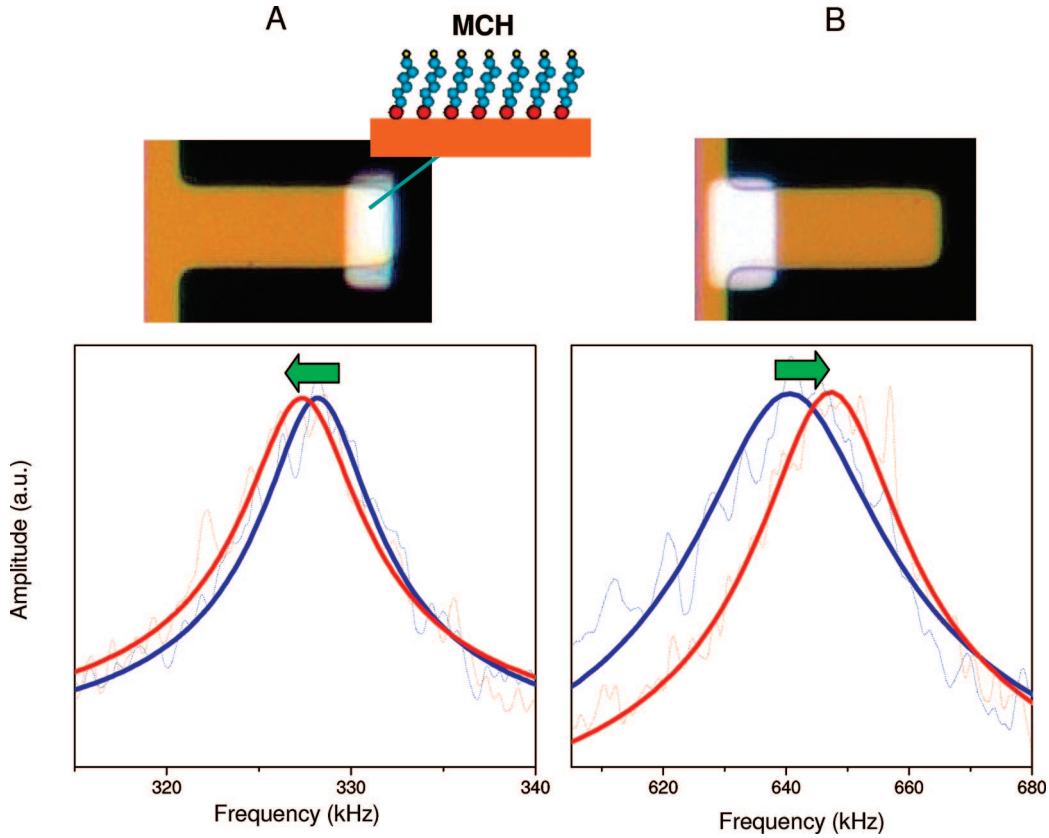

Figure 2. (A and B) Representative resonance peaks of the cantilevers with the Au area at the tip (A) and at the fixed end (B) before (blue line) and after adsorption of MCH (red dashed peaks). Optical images of the cantilevers and schematic of the MCH self-assembled monolayer are also show on top of the graphs. The resonance peaks are obtained from the fitting of the Fourier transform of the signal noise with the harmonic oscillator model.

To illustrate how the dual nanomechanical array responds to molecular adsorption, we exposed the array to mercaptohexanol (MCH), a 0.8 nm long alkylthiol ended in a hydroxyl group. The MCH molecules diluted in ultrapure water self-assemble on the Au areas via the chemical bond between the Au and the thiol group.[14] Molecules weakly adsorbed on the cantilever are removed by rinsing in water. Figure 2 shows the characteristic shifts of the resonance peaks for the cantilevers with the Au areas at the free and fixed ends. As expected, the cantilevers with the Au area at the tip exhibit a decrease of the resonance frequency (Figure 2A). The measurements in about 15 cantilevers give a relative frequency shift of about $-0.27\% \pm 0.07\%$. As described below, the resonance frequency response in this configuration arises from the added mass, and the numerical calculations give a mass responsivity of about 140 ag per Hz. This value implies a surface density of about 10^{15} molecules/cm^2 close to the reported values for alkanethiols.[14] Strikingly, the resonance frequency of the cantilevers with the Au area at the fixed end significantly increased (Figure 2B). The relative resonance frequency shift was $0.90\% \pm 0.27\%$. The positive shift of the resonance frequency cannot be explained by the added mass effect. We will return to this point later; however, let us advance that the property that gives this resonance response is the two-dimensional elasticity of the monolayer.

(14) Wink, Th.; van Zuilen, J.; Bult, A.; van Bennekom, W. P. *Analyst* **1997**, *122*, 43R–50R.

Detection of DNA Hybridization. The finding described above suggests that nanomechanical resonators can be applied for biosensing based on a double signature: the added mass reported by the cantilevers with the Au area at the tip and the monolayer elasticity reported by the cantilevers with the Au area at the fixed end. To demonstrate this hypothesis, we apply the cantilever arrays for measuring Watson−Crick pairing of cantilever-grafted single-stranded DNA (ssDNA) with complementary DNA. The arrays were functionalized with a 16mer ssDNA derivatized with a thiol linker that strongly binds to the gold. To assess the specificity of the measurements, the cantilevers were first exposed to a noncomplementary ssDNA (NC-DNA) and then to the complementary ssDNA (C-DNA). The adsorption of the NC-DNA prior to the detection of the C-DNA has a twofold purpose. First, since the length and charge of both kinds of DNA molecules are the same, a similar nonspecific adsorption on the cantilever surface is expected. Therefore, the NC-DNA acts as an excellent blocking molecule for detecting the hybridization signal corresponding with the C-DNA. Second, the measurements of the sensor response to the nonspecific binding of NC-DNA is critical for the design of selective nucleic acid sensors.

Figure 3 shows the relative resonance frequency shifts obtained after the exposure to NC-DNA and C-DNA. Mean values and deviations are from the experimental measurements in 70 cantilevers and from four different chips. For the cantilevers with the Au area at the tip, the relative resonance frequency shifts upon

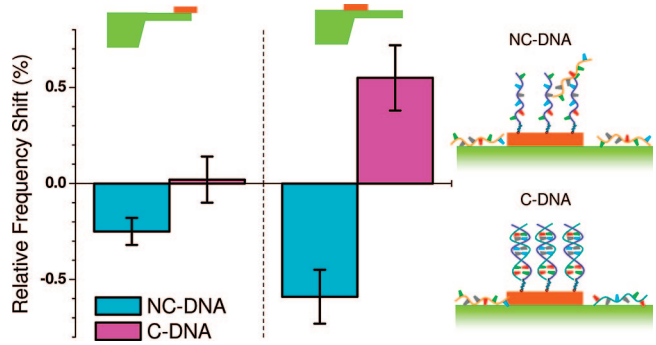

Figure 3. Mean relative resonance frequency shift of the cantilevers upon exposure to noncomplementary DNA, NC-DNA (cyan bars), and subsequent exposure to complementary DNA, C-DNA (magenta bars). The data are split into cantilevers with the Au area at the tip (left) and cantilevers with the Au area at the fixed end (right). The data arise from 70 cantilevers. A schematic of the adsorption step is shown at the right.

NC-DNA and C-DNA were −0.25% ± 0.10% and +0.03% ± 0.12%, respectively. The significant response induced by the NC-DNA is related to the nonspecific binding of these molecules on the cantilever. However, the C-DNA target provides a negligible resonance frequency shift, which indicates that the molecular recognition between complementary molecules cannot be distinguished. In the case of the cantilevers with the Au area at the fixed end, the mean resonance frequency shifts for NC-DNA and C-DNA were −0.59% ± 0.14% and +0.55% ± 0.17%, respectively. As shown above, the significant negative shift of the resonance frequency after the NC-DNA adsorption arises from the nonspecific adsorption that blocks the cantilever surface to nonspecific binding events of the C-DNA. Importantly, the C-DNA target gives a significant resonance frequency shift with a positive sign that is opposite to that given by the NC-DNA.

Fluorescence Characterization of the DNA Hybridization on the Cantilevers. The understanding of the response of the nanomechanical resonators requires knowing how the molecules are distributed along the cantilever. For this purpose, we used fluorescence confocal microscopy for imaging the location of fluorescein-labeled NC-DNA and C-DNA molecules on cantilevers previously functionalized with the thiol-derivatized ssDNA probes. Figure 4 shows the relative cross sections of the fluorescence signal along the cantilever longitudinal axis for the NC-DNA (triangles) and C-DNA (circles). For the cantilevers with the Au area at the tip, the NC-DNA and C-DNA fluorescence signals were significantly higher in the gold than in the silicon nitride (Figure 4, parts A and C). In addition, the fluorescence signals in the Au area were similar for both sequences. This result is consistent with the negligible resonance frequency shift obtained between the C-DNA and NC-DNA adsorptions. The main difference between the fluorescence of both DNA molecules was the distribution pattern on the Au area. The C-DNA fluorescence signal was uniformly distributed on the Au area at the tip, whereas the NC-DNA fluorescence signal increased with the distance until reaching a maximum near the free cantilever end. In consistency with the selectivity shown in the resonance frequency response, the cantilevers with the Au area at the fixed end showed drastic differences between the fluorescence of the NC-DNA and C-DNA (Figure 4, parts B and D). The C-DNA fluorescence signal was higher and located at the Au area, which indicates the successful formation of the DNA duplexes. The NC-DNA fluorescence signal was significantly weaker at the Au area, and its maximal value was located near the cantilever tip.

We found that, in general, the fluorescence of the NC-DNA molecules increases as the adsorption sites are closer to the cantilever tip (Figure 4, parts A and B). This phenomenon can be explained in terms of diffusion-assisted transport.[15,16] Basically, the large base area competitively captures DNA molecules from the vicinity of the cantilevers, depleting the adsorption on the cantilever. Thus, the DNA molecules are more efficiently collected by the cantilever tip. This effect degrades the specificity of the measurements with cantilevers where the sensing region is placed near the cantilever tip to maximize the mass sensitivity. On the contrary, the diffusion transport effect can be used to increase the selectivity by confining the molecular recognition reactions near the cantilever fixed end.

Origin of the Resonance Frequency Response. We can now address the analysis of the mechanisms responsible for the measured resonance frequency shifts. The governing equation for small deflections (w) of a thin cantilever plate in one dimension along its longitudinal axis can be approximated as $[D(x)w_{,xx}]_{,xx} + [\lambda_c + \lambda_a(x)]w_{,tt} = 0$, where D is the effective flexural rigidity, λ is the mass per unit length, the subscripts c and a denote the cantilever beam and the adsorbed layer, and the subscript-comma notation is used for partial derivatives in time (t) and 1D space (x). The equation indicates that a shift of the resonance frequency upon adsorption mainly arises from the variations in the flexural rigidity and mass of the cantilever. To calculate the resonance frequency we have applied a numerical approximation based on the Rayleigh's approximation previously developed elsewhere.[17]

For the cantilevers with the Au area at the tip, the contribution of the mechanical properties of the DNA film to the total resonance frequency shift is at least 2 orders of magnitude smaller than the mass contribution. The significant change of the resonance frequency after the NC-DNA exposure is consistent with the significant fluorescence signal found for this sequence on the Au area. Moreover, the small difference in fluorescence

(15) Squires, T. M.; Messinger, R. J.; Manalis, S. R. *Nat. Biotechnol.* **2008**, *26*, 417–426.
(16) Gupta, A. K.; Nair, P. R.; Akin, D.; Ladisch, M. R.; Broyles, S.; Alam, M. A.; Bashir, R. *Proc. Natl. Acad. Sci. U.S.A.* **2006**, *103*, 13362–13367.
(17) Tamayo, J.; Ramos, D.; Mertens, J.; Calleja, M. *Appl. Phys. Lett.* **2006**, *89*, 224104.

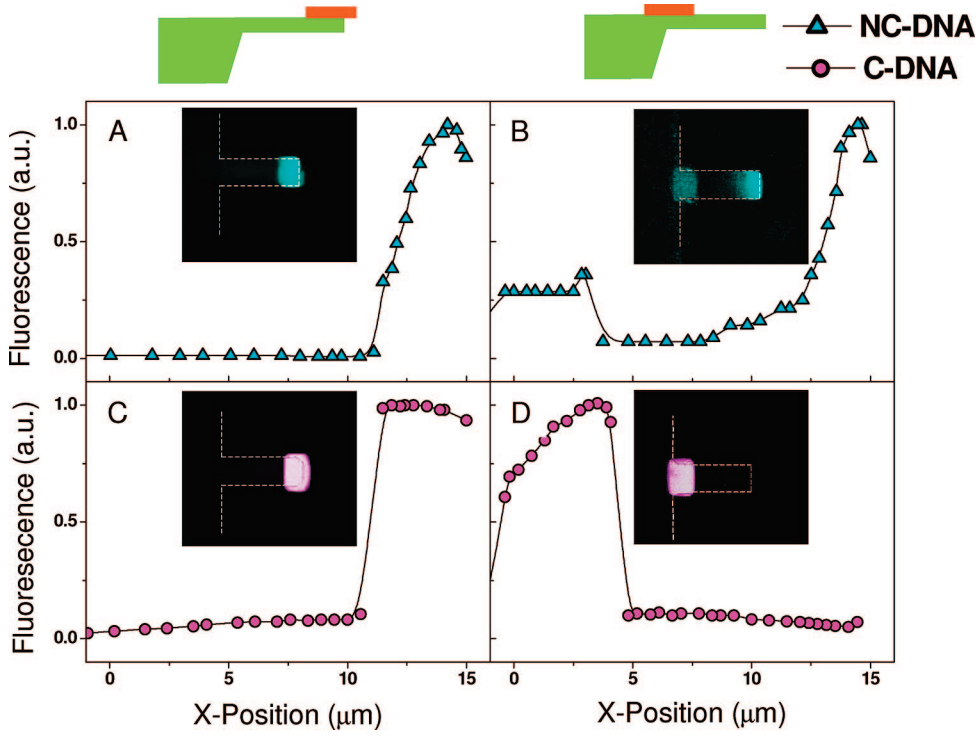

Figure 4. Mean fluorescence signal as a function of the longitudinal cantilever coordinate (*X*-position) for cantilevers with the Au paddle at the tip (A and C) and at the fixed end (B and D) exposed to noncomplementary DNA (NC-DNA) (A and B) and complementary DNA (C-DNA) (C and D). The cantilevers were previously functionalized with thiolated ssDNA. The fluorescence was normalized to the maximum value. The NC-DNA and C-DNA molecules were labeled with fluorescein. The fluorescence images are also shown as insets.

between the NC-DNA and C-DNA is consistent with the negligible resonance frequency shift produced after the hybridization step. The mass detection limit of these devices depends on the frequency noise. For a bandwidth of 0.1 Hz, the fundamental frequency noise is of about 5 Hz, that implies a mass detection limit of 0.4 fg.[18] However, the electrical noise in our measurements sets the frequency noise in 100−200 Hz, which corresponds to a mass detection limit of about 20−30 fg. We have investigated if the mass sensitivity can be enhanced by making the measurements in vacuum, where Q is 2000−3000 and the experimental frequency noise was of few hertz. The mean values of the resonance frequency shift were almost identical to those found in air. However, the resonance frequency shifts obtained after DNA hybridization showed a significant deviation of about 100 Hz between different cantilevers, which implies the mass detection limit is of about 10 fg. Therefore, the limiting source of noise arises from the random nonspecific adsorption events of the DNA molecules and other possible contaminants coming into play during the incubation process.

The cantilevers with the Au area at the fixed end exhibit a more intriguing response. Thus, all the discussion hereinafter will be focused on these structures. We found that the resonance frequency of these cantilevers largely decreased upon nonspecific adsorption of NC-DNA and increases upon hybridization with the C-DNA target. The negative resonance frequency shift due to the NC-DNA is related to the mass added by the preferential adsorption near the cantilever tip. However, the hybridization is confined to the cantilever fixed end; thereby the response arises from the induced changes in the flexural rigidity of the cantilever. In fact, the calculations indicate that the mass contribution to the frequency shift is 50−100 times smaller. The stiffness mechanism has been demonstrated as very effective for detecting bacteria adsorption.[19,20] In this case, the resonance frequency increased due to the elastic stiffness of the bacteria adsorbed on the fixed end of a microcantilever. However, the determination of the stiffness of a biomolecule monolayer poses a formidable challenge. The stiffness of the monolayer cannot only be accounted by the mechanical properties of the individual biomolecules, as it occurs in volumetric objects. Surface phenomena play a significant role in the elasticity of the monolayer, and it can significantly influence on the resonance frequency of ultrathin cantilevers. The surface mechanisms that can change the flexural rigidity of the cantilever have been split into two terms. The first mechanism arises from the intrinsic Young's modulus of the grafted DNA monolayer on the directions parallel to the surface. The Young's modulus arises from the long- and short-range interactions between the DNA chains and the potential between sulfur-bound gold atoms on the surface. This mechanism includes the effect referred by other authors to as strain-dependent surface stress.[21] In general, this mechanism can be quantified by the second derivative of the surface energy with respect to the longitudinal strain of the cantilever excluding the bending effects. There are scarce measurements of the Young's modulus of organic and biological

(18) Tamayo, J.; Calleja, M.; Ramos, D.; Mertens, J. *Phys. Rev. B* **2007**, *76*, 180201.

(19) Ramos, D.; Tamayo, J.; Mertens, J.; Calleja, M.; Zaballos, A. *J. Appl. Phys.* **2006**, *100*, 106105.

(20) Ramos, D.; Tamayo, J.; Mertens, J.; Calleja, M.; Villanueva, L. G.; Zaballos, A. *Nanotechnology* **2008**, *19*, 035503.

(21) Lu, P.; Lee, H. P.; Lu, C.; O'Shea, S. J. *Phys. Rev. B* **2005**, *72*, 085405.

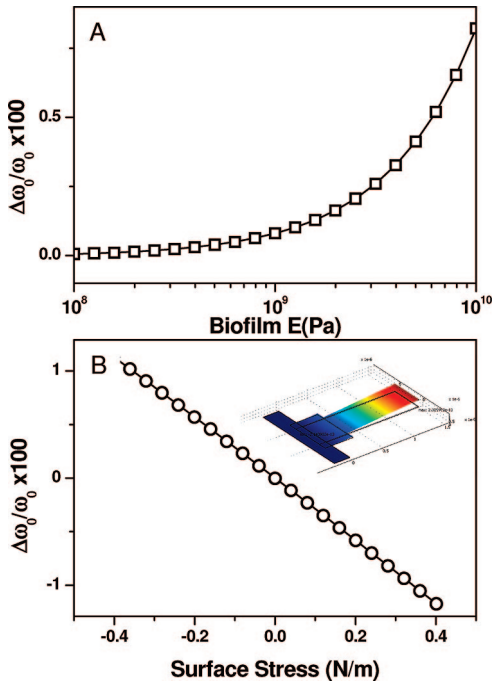

Figure 5. (A) Numerical calculation based on the one-dimensional beam equation of the influence of the Young's modulus of the biolayer on the relative frequency shift of the cantilever with the Au paddle at the fixed end. In this calculation the effect of the mass on the resonance is lower than 100 ppm; therefore, it may be neglected. (B) Finite element calculations of the relative resonance frequency shift of a cantilever with the Au area at the fixed end as a function of the surface stress. The inset shows the mesh used in the finite element simulation. The values used in the calculations were 78 GPa for the Young's modulus of gold, 2900 kg/m^3 for the SiN mass density, 19 300 kg/m^3 for the Au mass density, 0.27 for the SiN Poisson coefficient, and 0.44 for the Au Poisson coefficient. The Young's modulus used for the SiN was 120 GPa based on resonance frequency measurements. The cantilever dimensions used in the simulations were those of the fabricated cantilevers: a length of 15 μm, a width of 6 μm, and a thickness of 100 nm. The Au paddle at the fixed end was 5 μm long and 25 nm thick.

monolayers. In our calculations, we have found a significant effect of monolayer elasticity on the resonance frequency for Young's modulus above 1 GPa (Figure 5A). This value is close to the values reported for organic and biomolecule monolayers in the dry state.[17,22]

The second mechanism that can change the flexural rigidity of the cantilever near the fixed end is related to the in-plane stresses generated near the cantilever clamp upon adsorption. This mechanism depends on both the cantilever geometry and the adsorption-induced surface stress. The effect on the resonance frequency for a uniform cantilever beam has recently been modeled by Lachut and Sader[23] and is given by $\Delta\omega/\omega_0 \sim -(b/L)(b/h)^2\sigma/Eh$, where b is the cantilever width, h is the cantilever thickness, L is the cantilever length, E is the Young's modulus. This effect becomes significant as the cantilevers are getting thinner and the ratio between L/b is low. We have performed finite element simulations to study the effect of the surface stress on the resonance frequency of our cantilevers (Figure 5B). The resonance frequency shows a significant linear dependence with the surface stress.

We have measured the surface stress induced by the DNA hybridization by measuring the change of curvature of gold-coated silicon microcantilevers.[2] The mean value of the hybridization-induced surface stress was of −0.01 N/m, which gives an insignificant resonance frequency shift. Therefore, the response of the cantilevers with the Au area at the fixed end is attributed to the stiffening of the DNA monolayer upon hybridization. Reported measurements carried out with the surface force apparatus indicate that the shear modulus of thiolated ssDNA monolayers significantly increases upon hybridization.[22] It is well-known that dsDNA monolayers are significantly stiffer than single-stranded ssDNA monolayers. This is because ssDNA has a much shorter persistence length (≈0.75 nm) than dsDNA (≈50 nm).[24] However, we notice that the surface stress contribution cannot be neglected in other cases, such as the adsorption of self-assembled monolayers that generate a significant surface stress. In those cases, the two-dimensional elasticity and surface stress contribute to the resonance frequency shift.

CONCLUSIONS

We have demonstrated that, by using arrays combining resonating ultrathin cantilevers with confining sensing regions alternately placed at the free and the fixed ends, a double signature of the adsorbed molecules can be obtained. We have applied this concept for detection of DNA. The cantilevers with the Au area at the tip mainly act as mass sensors and gave a limited sensitivity for this application. However, the cantilevers with the Au area near the fixed end provided higher sensitivity and good selectivity to distinguish the specific DNA target from nonspecific DNA molecules. This selectivity is enhanced by the favorable diffusive flux of molecules toward the cantilever tip. These cantilevers are mainly sensitive to changes in the flexural rigidity of the cantilever near the clamp. Further theoretical and experimental developments are still needed in order to elucidate the intermolecular interactions responsible of the variation of the flexural rigidity due to the adsorption of biomolecule monolayers. However, the results indicate that the combination of nanomechanical resonators with different geometries that make them sensitive to different properties of the adsorbates is a promising route for ultrasensitive and specific detection of biological targets.

ACKNOWLEDGMENT

D.R. acknowledges the fellowship funded by the Autonomous Community of Madrid (CAM). E.G.-S. acknowledges a fellowship funded by C.S.I.C. M.A.-H. acknowledges a contract funded by the Spanish Ministry of Science. J.T. and M.C. acknowledge financial support by the Spanish Ministry of Science under Grant Nos. TEC2006-10316 and CSD 2007-00010 and by the Autonomous Community of Madrid under contract S-0505/MAT-0283. All the authors acknowledge J. Mertens for his helpful suggestions.

Received for review November 14, 2008. Accepted January 28, 2009.

AC8024152

(22) Cho, Y.-K.; Kim, S.; Lim, G.; Granick, S. *Langmuir* **2001**, *17*, 7732–7734.
(23) Lachut, M. J.; Sader, J. E. *Phys. Rev. Lett.* **2007**, *99*, 206102.
(24) Hagan, M. P.; Majumdar, A.; Chakraborty, A. K. *J. Phys. Chem. B* **2002**, *106*, 10163–10173.